AD142811

Department of the Navy
Bureau of Ordnance
Contract NOrd-16200
Task 1

AN EXPERIMENTAL DETERMINATION OF DYNAMIC COEFFICIENTS FOR THE BASIC FINNER MISSILE BY MEANS OF THE ANGULAR DYNAMIC BALANCE

Taras Kiceniuk

Hydrodynamics Laboratory
CALIFORNIA INSTITUTE OF TECHNOLOGY
Pasadena, California

Report No. E-73.3
June 1957

Approved by
Haskell Shapiro

Department of the Navy
Bureau of Ordnance
Contract NOrd-16200
Task I

AN EXPERIMENTAL DETERMINATION OF DYNAMIC CHARACTERISTICS FOR THE BASIC FINNER MISSILE BY MEANS OF THE ANGULAR DYNAMIC BALANCE

Taras Kiceniuk

Hydrodynamics Laboratory
California Institute of Technology
Pasadena, California

Report No. E-73.3
June 1957

Approved by:
Haskell Shapiro

INTRODUCTION

Equipment developed in this Laboratory permits the determination of eight of the dynamic coefficients useful in describing the force and moment reactions on a submerged body moving in water. These coefficients comprise the partial derivatives of moment (about the yaw axis) and of force (in the horizontal plane, and perpendicular to the longitudinal axis) with respect to velocity and acceleration components in specified directions. So long as the instantaneous angles of attack are small and scale effects are absent, these coefficients have constant values. A complete list of coefficients is given in Ref. (1), as are definitions, sign conventions and formulas for making the coefficients nondimensional. The eight coefficients tabulated below are those pertinent to lateral translation and rotation about the yaw axis for a body of revolution:

N_r' coefficient of rotary moment derivative

$N_{\dot{r}}'$ virtual moment of inertia coefficient (angular acceleration)

N_v' coefficient of static moment derivative

$N_{\dot{v}}'$ virtual moment of inertia coefficient (lateral acceleration)

Y_r' coefficient of rotary force derivative

$Y_{\dot{r}}'$ virtual inertia coefficient (angular acceleration)

Y_v' coefficient of static force derivative

$Y_{\dot{v}}'$ virtual inertia coefficient (lateral acceleration)

where the prime indicates that the coefficients are in dimensionless form.

It is the purpose of the experimental program undertaken at this Laboratory to determine the numerical values of the above quantities for

the Basic Finner missile (Fig. 1). Because of the required differences in the experimental methods, however, the program was divided into two parts. This report deals only with Part 1, and is restricted to the following quantities: N_r', N_v', Y_r', Y_v', and the linear combinations $N_r' - N_v'$ and $Y_r' - Y_v'$. Remaining quantities will be the subject of another report.

APPARATUS

The procedure used to obtain the dynamic moment coefficients is based on the measurement of the amplitude ratio and phase angle of the model while it is oscillated at a known frequency in the moving stream of water. For this purpose the Angular Dynamic Balance was used, in conjunction with the High Speed Water Tunnel at this Laboratory. A complete discussion and description of the equipment is given in Ref. 2, but a brief summary is given here:

The balance can be regarded as consisting of several separate functional components (Fig. 2). The first of these is the platform - platform drive assembly. This unit consists of a platform to which can be imparted a small angular oscillation of known amplitude and controllable frequency. To it is coupled the spindle-model assembly which is free to rotate on ball bearings and which is provided with a water seal to prevent leakage of tunnel water to the outside. The coupling member is a calibrated torsion spring of controllable stiffness. Two mirror-lens systems, one of which is carried by the driving platform and the other by the spindle, enable the observer to measure the angular deflections of each of these components with respect to ground. By projecting the image of a pulsing light source (triggered by contacts on the drive assembly) the angular deflection at a given instant

in the cycle can be measured. The contactor body is rotated through known angular increments and the deflections taken. By plotting these data and by representing the observed motions in Fourier series, the amplitude and phase angles of the fundamental motion of both driver and spindle can be determined.

A self-contained lateral force balance, using bonded strain gages, serves as the center section of the model assembly. This unit measures the instantaneous side force acting on the model and relates it to the instantaneous position of the driving platform.

THEORETICAL ANALYSIS

Up to this point the balance has been regarded as a harmonic oscillator which permits complete analysis of the motions of both the driving platform and of the spindle-model assembly. By running the balance in air, and by performing the necessary computations, the spindle-model assembly is found to possess a certain moment of inertia and little or no damping with respect to ground. Similarly the internal (lateral force) balance shows that the center of gravity of the model assembly coincides very closely with the axis of angular oscillation. This fact is indicated by the absence of any measured periodic lateral force in the presence of the angular motion.

When the tunnel is filled with water which is moving relative to the model, the behavior of the model is strikingly different. Analysis of the motions of the platform and spindle shows that the spindle "sees" a larger mass, coupled to ground through a spring, and possessing a degree of damping with respect to ground. This spring can either aid or oppose the model displacement and the damping can be positive or negative. In similar fashion, the internal balance shows that periodic side forces are present which behave

as though caused by oscillating a larger mass, coupled to ground by a spring, and also possessing some amount of damping.

The relationship between the instantaneous forces and moments exerted by the spindle on the model and the resulting motion of the model can be given in terms of the effective physical parameters of the system and the angular displacement β_o of the model:

$$m\ddot{\beta}_o - b\dot{\beta}_o - k\beta_o = Y_s \qquad (1)$$

$$I\ddot{\beta}_o + B\dot{\beta}_o + K\beta_o = N_s \qquad (2)$$

where the sign convention has been chosen to facilitate final expression of the desired hydrodynamic coefficients. In these equations

m = total apparent mass of the model

b = lateral force damping coefficient of model with respect to ground

k = effective lateral spring rate with respect to ground

I = total effective moment of inertia of model in water

B = torsional damping moment coefficient of model

K = effective torsional spring rate with respect to ground

These apparent physical properties of the model and model-spindle assembly are a result of the hydrodynamic forces acting on the model. For the small oscillations executed by the model and for the small instantaneous angles of attack, the hydrodynamic reactions can be regarded as comprising the sum of the individual reactions arising from displacement, velocity, and acceleration in the direction of motion. Letting N equal the total hydrodynamic moment acting on the body about the yaw axis and Y equal the total hydrodynamic lateral force, then

$$N = N_u u + N_{\dot{u}}\dot{u} + N_v v + N_{\dot{v}}\dot{v} + N_r r + N_{\dot{r}}\dot{r} \qquad (3)$$

and

$$Y = Y_u u + Y_{\dot{u}} \dot{u} + Y_v v + Y_{\dot{v}} \dot{v} + Y_r r + Y_{\dot{r}} \dot{r}$$

where subscripts indicate partial derivatives in accordance with the list of symbols on page 13 and

$U \approx u$ velocity of body axis relative to fluid at infinity.

$r = \dot{\beta}_o$ angular velocity of model about the yaw axis.

$v \approx -U \beta_o$ component of velocity of body axis relative to fluid in the direction perpendicular to the longitudinal axis and in the horizontal plane.

$\dot{v} \approx -U \beta_o$ component of acceleration of body relative to fluid in the direction perpendicular to the longitudinal axis and in the horizontal plane.

Since the body in question possesses rotation symmetry, the following terms must vanish for constant u.

$N_u u$, $N_{\dot{u}} \dot{u}$, $Y_u u$, and $Y_{\dot{u}} \dot{u}$.

Equation (3) can therefore be rewritten in as

$$N = N_{\dot{r}} \ddot{\beta}_o + (N_r - N_{\dot{v}} U) \dot{\beta}_o - N_v U \beta_o$$

$$Y = Y_{\dot{r}} \ddot{\beta}_o + (Y_r - Y_{\dot{v}} U) \dot{\beta}_o - Y_v U \beta_o \qquad (4)$$

For the present case, the center of gravity of the test body was very nearly at the center of rotation, so that all side force reactions were hydrodynamic in origin, or

$$Y = - Y_s \qquad (5)$$

Also, the moment reaction on the spindle due to damping and displacement in air was zero; therefore the only nonhydrodynamic reaction was due to the moment of inertia of the spindle-model assembly, or

$$N = I_b \ddot{\beta}_o - N_s \tag{6}$$

so that by combining terms in (1), (2) and (4), and substituting in (5) and (6), the hydrodynamic coefficients can be identified with the effective physical quantities characteristic of vibrating mass systems:

$$\begin{aligned} m &= -Y_{\dot{r}} \qquad b = (Y_r - Y_v U) \qquad k = -Y_v U \\ I_f &= -N_{\dot{r}} \qquad B = (N_r - N_v U) \qquad K = N_v U \end{aligned} \tag{7}$$

where U is the constant relative fluid velocity at a great distance from the body.

The experimental problem then reduces to one of finding the numerical values of these effective physical constants, m, k, I_f, B, and K, by whatever means available. The dynamic balance and its accessory instrumentation provides this means. If the equations of motion for the system are formulated, the following pair of equations is obtained:

$$\begin{aligned} I_s \ddot{\beta}_1 + B_s \dot{\beta}_1 &= K_d(\beta_2 - \beta_1) - K_s (\beta_1 - \beta_o) \\ I \ddot{\beta}_o + B \dot{\beta}_o + K \beta_o &= K_s (\beta_1 - \beta_o) \end{aligned} \tag{8}$$

where the symbols are as defined on page 12 and as shown in the equivalent linear analogy of the moment measuring apparatus in Fig. 2. From these expressions can be obtained the steady-state solution

$$\left[\frac{K_s + K}{K_s} - \frac{I\omega^2}{K_s} + \frac{i\omega B}{K_s}\right]^{-1} = \frac{K_d + K_s}{K_s} - \frac{I_s \omega^2}{K_s} + \frac{i\omega B_s}{K_s} - \frac{K_d A_2}{K_s A_1}\left[\cos(\delta_2 - \delta_1) - i \sin(\delta_2 - \delta_1)\right] \tag{9}$$

which reduces to

$$\left[\frac{K_s + K}{K_s} - \frac{I\omega^2}{K_s} + \frac{I\omega B}{K_s}\right]^{-1} = \frac{K_d + K_s}{K_s} - \frac{K_d A_2}{K_s A_1}\left[\cos(\delta_2 - \delta_1) - i \sin(\delta_2 - \delta_1)\right]$$

when terms containing the negligible quantities I_s and B_s are dropped.

The real part of this equation identifies the in-phase component and the imaginary part identifies the quadrature component. From this expression the effective physical constants I, B, and K, can be found, according to the method to be described later. Similarly, the expression

$$\frac{A_o}{A_2}\left[\cos(\delta_o - \delta_2) - i \sin(\delta_o - \delta_2)\right] = -\frac{K_d}{K_s} +$$

$$\left[\frac{K_d + K_s}{K_s} - \frac{I_s\omega^2}{K_s} + \frac{i\omega B_s}{K_s}\right]\left[\cos(\delta_1 - \delta_2) - i \sin(\delta_1 - \delta_2)\right]$$

first reduces to

(10)

$$\frac{A_o}{A_2}\left[\cos(\delta_o - \delta_2) - i \sin(\delta_o - \delta_2)\right] = -\frac{K_d}{K_s} + \frac{K_d + K_s}{K_s}\left[\cos(\delta_1 - \delta_2) - \sin(\delta_1 - \delta_2)\right]$$

and can be solved to give the amplitude and phase angle of the model in terms of measurable quantities. This information is required for subsequent evaluation of the lateral forces measured by the internal strain gage balance assembly, since, with the present setup, the internal balance actually measures phase angle relative to the motion of the driving platform. The

lateral force is related to the effective physical constants, m, b, and k, through the steady-state relation

$$F\left[\cos\ \delta_f + i \sin \delta_f\right] = -\left[(K - m\omega^2) + i\omega b\right] A_o \qquad (11)$$

where F is the peak value of the lateral force and δ_f is the phase angle of this force relative to the motion of the model.

REDUCTION AND ANALYSIS OF DATA

Equation 9 is seen to be a complex expression of the form

$$\frac{1}{a + ib} = c + id \qquad (12)$$

which can be rationalized to yield

$$a = \frac{c}{c^2 + d^2} \quad \text{and} \quad b = -\frac{d}{c^2 + d^2} \qquad (13)$$

where

$$a = \left[(1 + \frac{K}{K_s}) - (\frac{I_f \omega^2}{K_s})\right]$$

$$b = \left[\frac{\omega B}{K_s}\right] \qquad (14)$$

$$c = \left\{1 + \frac{K_d}{K_s}\left[1 - \frac{A_2}{A_1}\cos(\delta_2 - \delta_1)\right]\right\}$$

$$d = \left[\frac{K_d}{K_s}\ \frac{A_2}{A_1}\ \sin(\delta_2 - \delta_1)\right]$$

By plotting a against ω^2 (Fig. 3) and measuring the slope (I/K_s) and

y-intercept $(1 + K/K_s)$ two of the equivalent physical constants are found in terms of the known spindle spring rate. Similarly, if b is plotted against ω (Fig. 4) the slope of the resulting lines is equal to B/K_s. An analagous treatment of the lateral force equation (11) in Figs. 5 and 6 yields the quantities m, b, and k. These equivalent physical parameters are then equated to the appropriate hydrodynamic coefficients according to Eq. (7) and nondimensionalized, as indicated in Ref. 1. The resulting dynamic coefficients have been plotted against Reynolds number in Figs. 7 to 12. The use of Reynolds number as the similitude parameter does not imply an a priori judgment that viscosity effects are paramount in determining the magnitude of these coefficients. Indeed, for the experimental setup available for this study, where the model size and fluid viscosity were fixed, the Reynolds number change indicates only a change in velocity.

The effect of the presence of the model support spindle and spindle shield was estimated by the image method. That is, supplementary runs were made with a dummy support spindle shield on the side of the model opposite the real support spindle and shield. This dummy did not touch the model. The data points taken with this image in place are indicated by solid symbols in the final curves. It is assumed that the presence of the dummy shield produces the same effect as the original functional spindle and spindle shield; hence the final curve is taken to be displaced an amount equal to the difference between the original runs and the image runs, and in the direction of the original runs. In some cases the presence of the image strut had no effect on the values of the coefficients; for these no image runs were plotted.

SUMMARY OF RESULTS

(1) N_r', Virtual Moment of Inertia Coefficient (Fig. 7):

This coefficient is nearly independent of velocity, as predicted by perfect fluid theory, and shows little or no sensitivity to the presence of the support spindle.

(2) N_v', Coefficient of Static Moment Derivative (Fig. 8):

This coefficient is a measure of the moment component due to velocity perpendicular to the longitudinal body axis. For small angles of yaw this is seen to be identical to the static moment rate, $d C_m/d\alpha$, and for this reason it serves as a good check on the experimental and computational procedures. The agreement between the values reported in Fig. 8 and those reported in Ref. (3) are very good, even as to the effect of the presence of the support spindle.

(3) $N_r' - N_{\dot{v}}'$. Combined Moment Coefficient (Fig. 9):

Actually a linear combination of the coefficient of Rotary Moment Derivative and the Virtual Moment of Inertia Coefficient (to lateral acceleration), cannot be resolved without further experiments, which are to be conducted at a later time.

(4) $Y_{\dot{r}}'$, Virtual Inertia Coefficient (angular acceleration) (Fig. 10):

This quantity is negligibly small in the presence of the ponderable value of Y_v'.

(5) Y_v', Coefficient of Static Force Derivative (Fig. 11):

The analog to item (2) above, can be identified with the slope of the static lift coefficient curve $\alpha\, C_L/d\alpha$ found by conventional static balance measurements. As with item (2), the agreement with previous static

measurements (Ref. 3) is excellent.

(6) $Y_r' - Y_v'$, Combined Lateral Force Coefficient (Fig. 12):

As with item (3), this coefficient cannot be completely analyzed until the second phase of this investigation is completed.

LIST OF SYMBOLS

The motion of the test body is restricted to the plane of yaw. The symbols used to describe this motion and the associated hydrodynamic reactions on the body are in the greater part identical to those recommended in the Technical and Research Bulletin N. 1-5 of the Society of Naval Architects and Marine Engineers titled "Nomenclature for Treating the Motion of a Submerged Body through a Fluid". These symbols are marked with an asterisk(*) in the following list.

The coefficients have been made non-dimensional in accordance with procedures outlined in the above publication. Dimensionless quantities are primed; all other quantities are in the pound-foot-second system of units.

*	A	cross section area of model
	A_0, A_1, A_2	peak half amplitudes of motion of body, support spindle and drive platform
	b	damping coefficient in Eq. (1)
	B	torsional damping coefficient in Eq. (2)
	B_s	torsional damping rate of spindle seal
	d	diameter of model
	F	peak magnitude of lateral force in the horizontal plane
	$i = \sqrt{-1}$	
	$I = I_b + I_f$	total effective moment of inertia of model in water (Eq. (2))
	I_b	moment of inertia of model
	I_f	apparent moment of inertia of model assembly due to hydrodynamic reactions
	I_s	moment of inertia of model-support spindle
	k	effective spring rate due to hydrodynamic reactions (Eq. (1))
	K	effective torsional spring rate due to hydrodynamic reactions (Eq.2)
	K_d	torsional spring rate of drive spring which couples the driving platform to the spindle-model assembly
	K_s	torsional spring rate of model support spindle
*	ℓ	length of body
	m	apparent mass of model due to hydrodynamic reactions (Eq. (1))

LIST OF SYMBOLS (cont'd)

* N — Hydrodynamic moment acting on the model

$N_s = -N$ — moment on body supplied by support spindle

* $N_r = N_r' \ (1/2\rho A d^2 U)$ — coefficient of rotary moment derivative

* $N_{\dot{r}} = N_{\dot{r}}' \ (1/2\rho A d^3)$ — virtual moment of inertia coefficient (angular acceleration)

* $N_v = N_v' \ (1/2\rho A d\, U)$ — coefficient of static moment derivative

* $N_{\dot{v}} = N_{\dot{v}}' \ (1/2\rho A d^2)$ — virtual moment of inertia coefficient (lateral acceleration)

$r = \dot{\beta}$ — angular velocity about the yaw axis

* U — velocity of body axis relative to fluid at infinity

* u — component of velocity of body axis relative to fluid in the direction parallel to the longitudinal axis

* v — component of velocity of body axis relative to fluid in the direction perpendicular to the longitudinal axis and in the horizontal plane

* Y — hydrodynamic lateral force acting on the model

$Y_s = -Y$ — lateral force on the model supplied by the support spindle

* $Y_r = Y_r' \ (1/2\rho A d U)$ — coefficient of rotary force derivative

* $Y_{\dot{r}} = Y_{\dot{r}}' \ (1/2\rho A d^2)$ — virtual inertia coefficient (angular acceleration)

* $Y_v = Y_v' \ (1/2\rho A U)$ — coefficient of static force derivative

* $Y_{\dot{v}} = Y_{\dot{v}}' \ (1/2\rho A d)$ — virtual inertia coefficient (lateral acceleration)

$\beta_o, \beta_1, \beta_2$ — angular displacement about the yaw axis of the model, spindle, and drive platform

$\delta_o, \delta_1, \delta_2$ — phase constant of the motion of the model, spindle, and drive platform

δ_f — phase angle of the lateral force relative to model motion

ρ — mass density of fluid

$\omega = 2\pi f$ — circular frequency; f = frequency in cycles per second

LIST OF REFERENCES

1. Kiceniuk, Taras, "Dynamic Coefficients of the Mk-13 Torpedo", California Institute of Technology, Hydrodynamics Laboratory Report No. E - 12.20, April 1957

2. Stallkamp, John A., "Measurement of Dynamic Coefficients of Ellipsoids", California Institute of Technology, Hydrodynamics Laboratory Report No. E - 35.4, September 1956.

3. Kermeen, R. W., "Static Force Coefficients of the Basic Finner Missile in Fully Wetted Flow", California Institute of Technology, Hydrodynamics Laboratory. Report E - 73.2, June 1957.

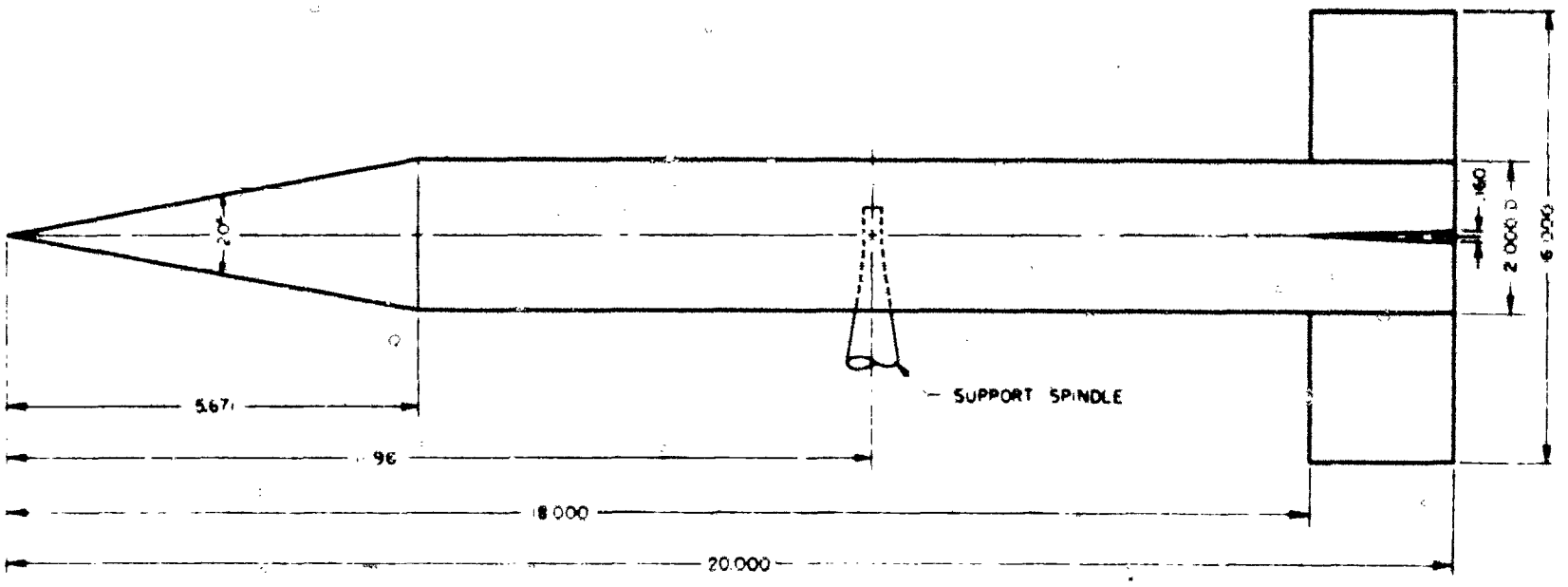

Fig. 1 - Important geometrical dimensions of the Basic Finner missile.

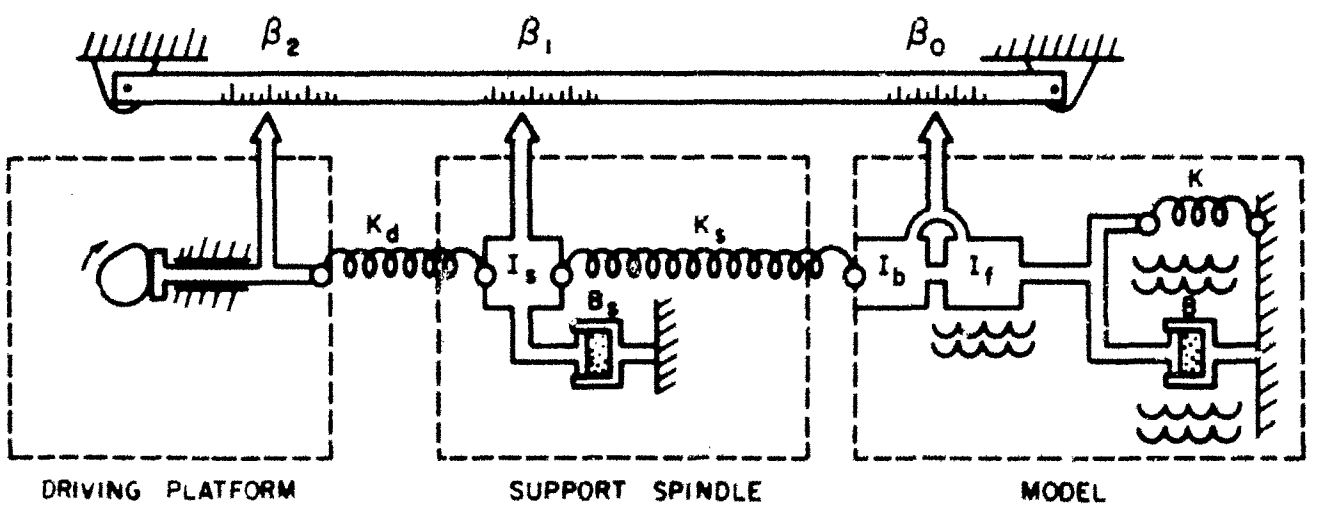

K_s TORSIONAL SPRING RATE OF SPINDLE
B_s TORSIONAL DAMPING RATE OF SPINDLE SEAL
I_s MOMENT OF INERTIA OF SUPPORT SPINDLE
I_b MOMENT OF INERTIA OF MODEL
I_f APPARENT MOMENT OF INERTIA
κ EFFECTIVE TORSIONAL SPRING RATE DUE TO HYDRODYNAMIC REACTIONS
B EFFECTIVE TORSION DAMPING RATE DUE TO HYDRODYNAMIC REACTIONS.

β_2 β_1 β_0 DISPLACEMENT OF PLATFORM, SPINDLE, MODEL
A_2 A_1 A_0 MAXIMUM AMPLITUDE OF PLATFORM, SPINDLE, MODEL
δ_2 δ_1 δ_0 PHASE CONSTANT OF PLATFORM, SPINDLE, MODEL

$$\beta_2 = A_2 \sin(\omega t - \delta_2)$$
$$\beta_1 = A_1 \sin(\omega t - \delta_1)$$
$$\beta_0 = A_0 \sin(\omega t - \delta_0)$$

Fig. 2 - Schematic diagram of dynamic balance driving platform and moment measuring components.

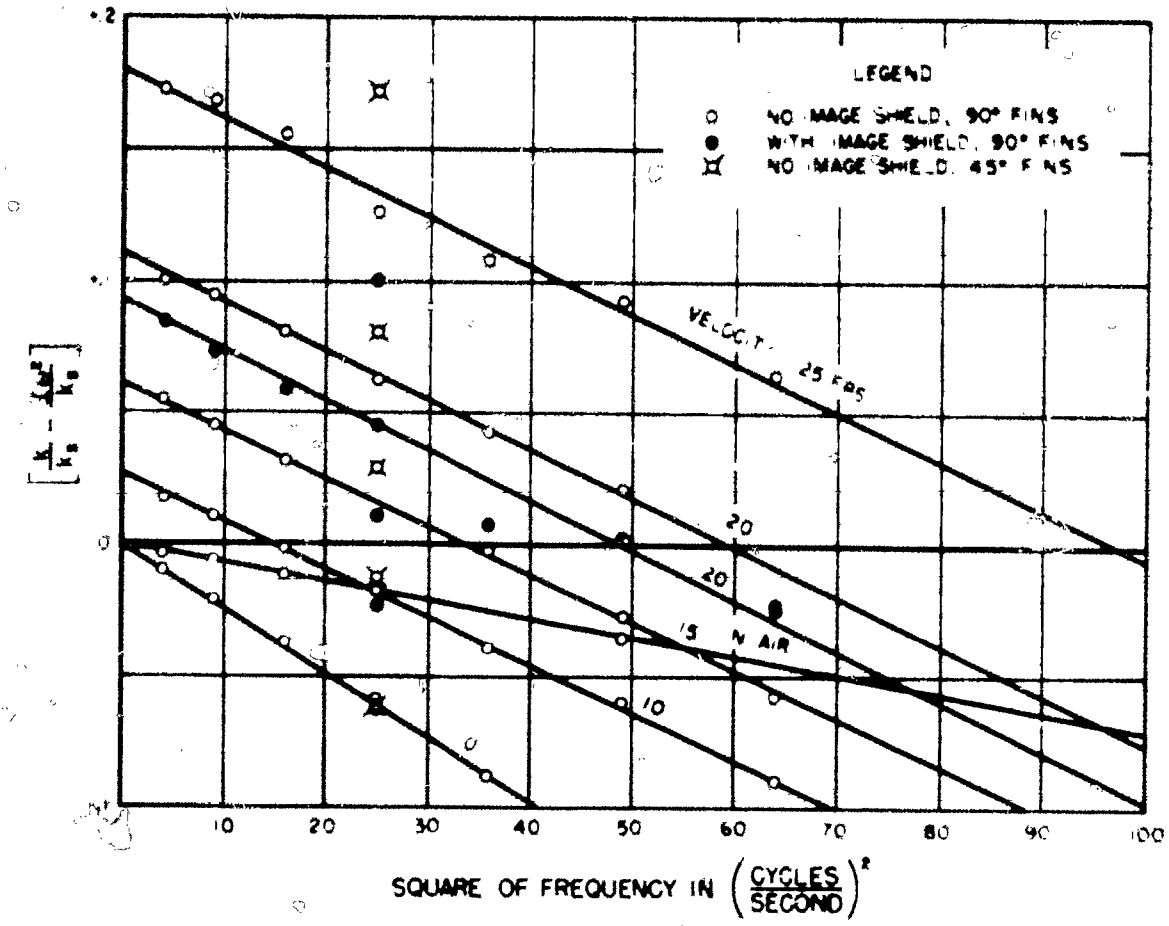

Fig. 3 - Moment data reduction plot: In-phase component (real part Eq. 9).

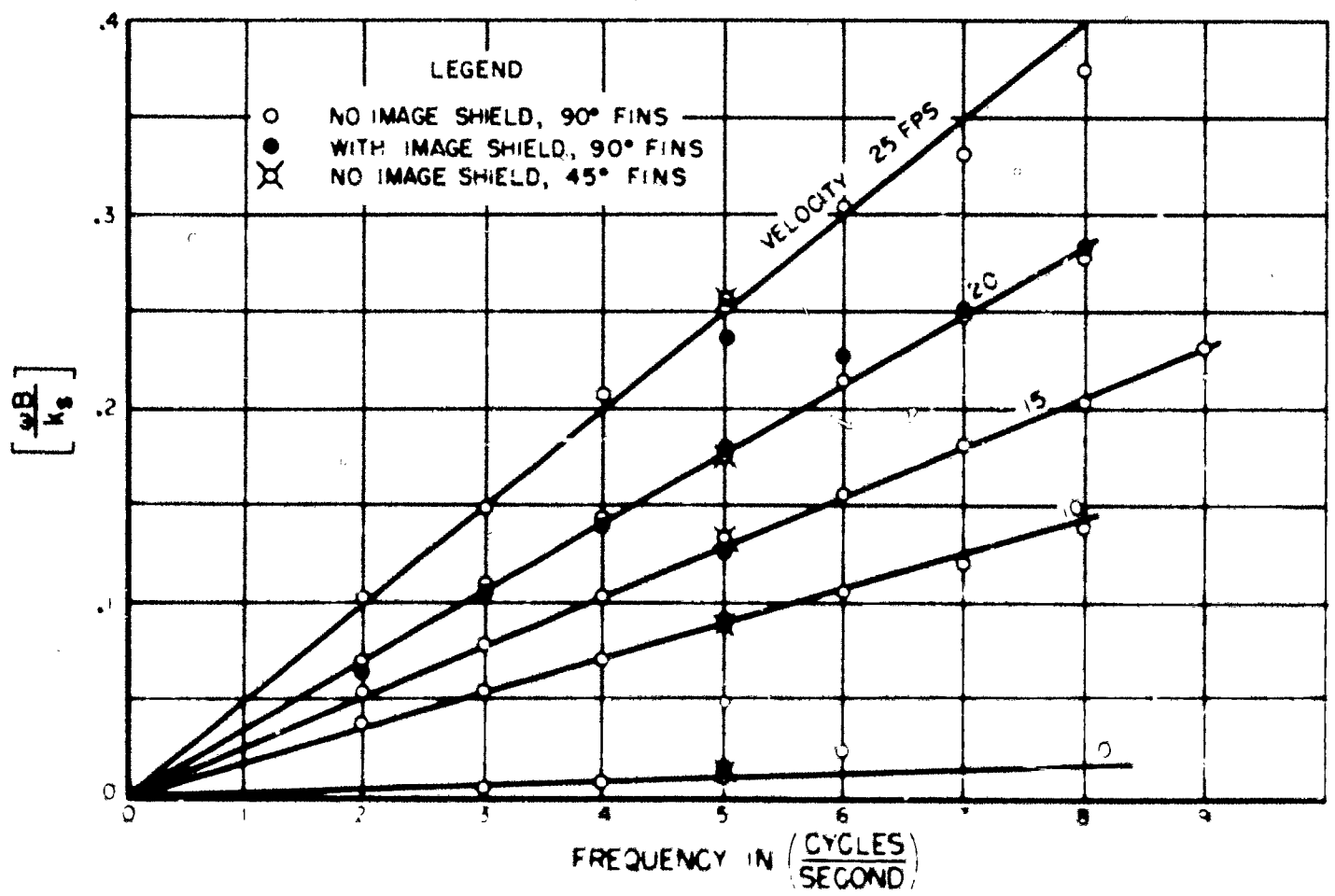

Fig. 4 - Moment data reduction plot: Quadrature component (imaginary part Eq. 9).

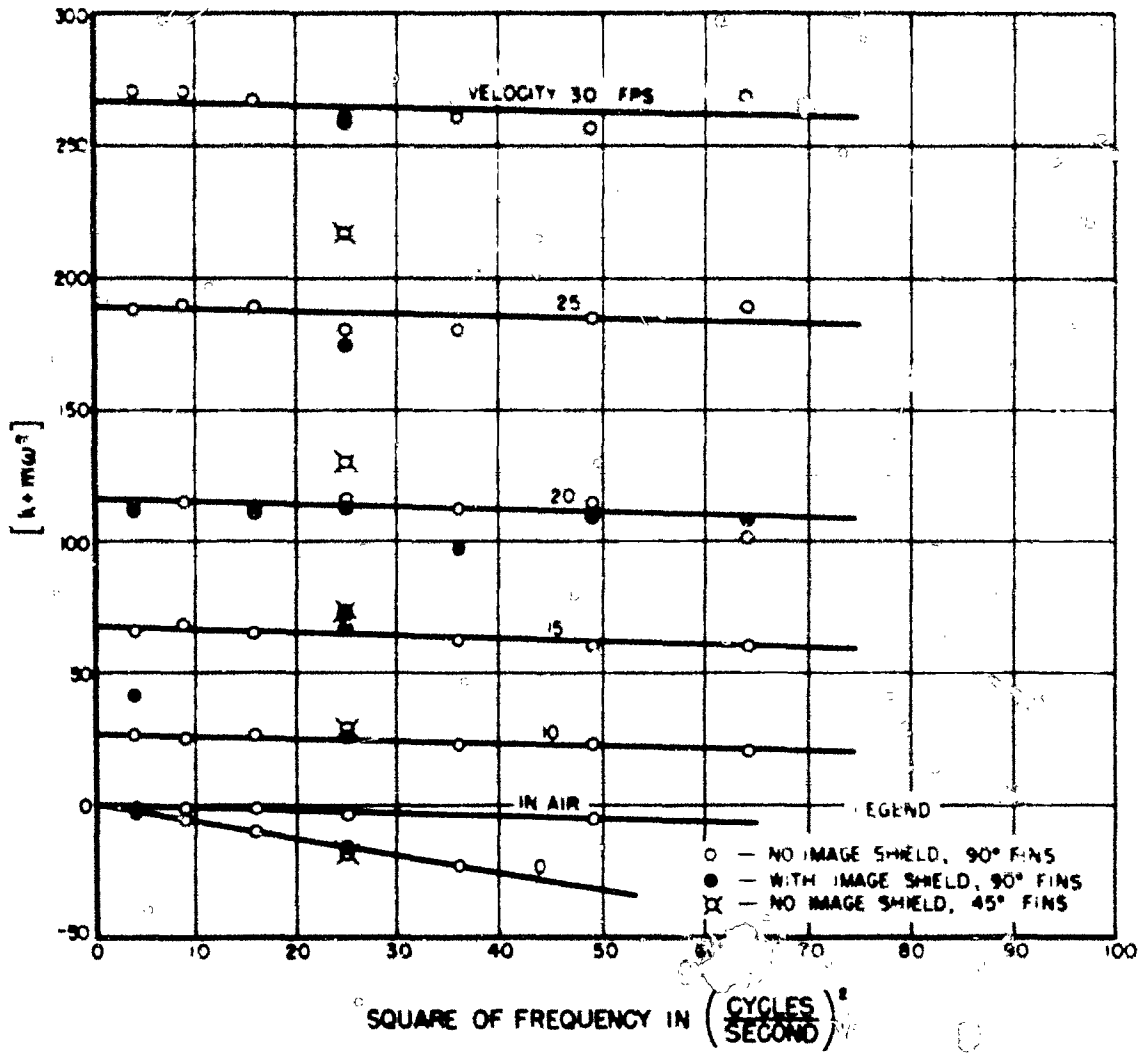

Fig. 5 - Lateral force data reduction plot: In-phase component (real part Eq. 11).

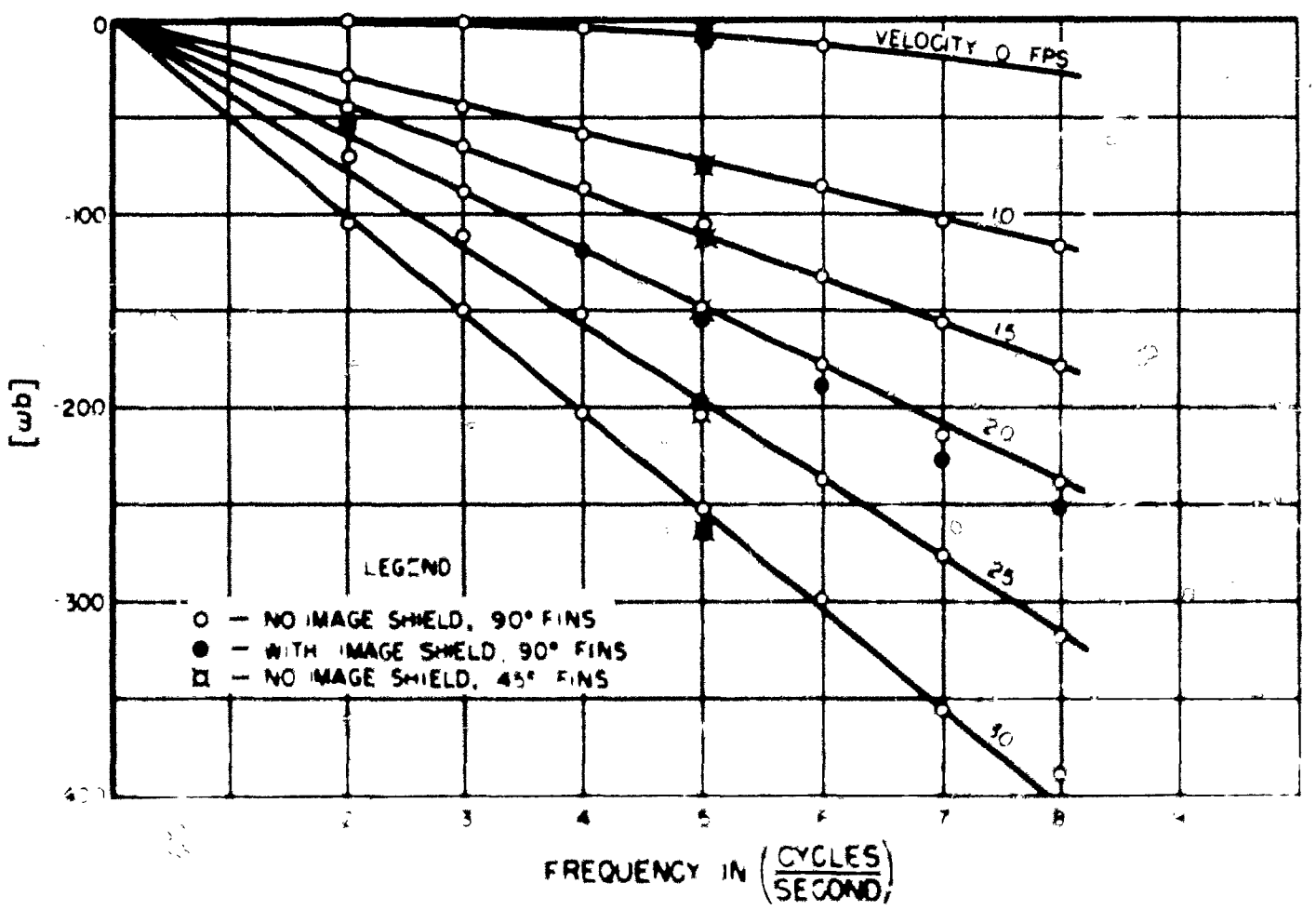

Fig. 6 - Lateral force data reduction plot: Quadrature component (imaginary part Eq. 11).

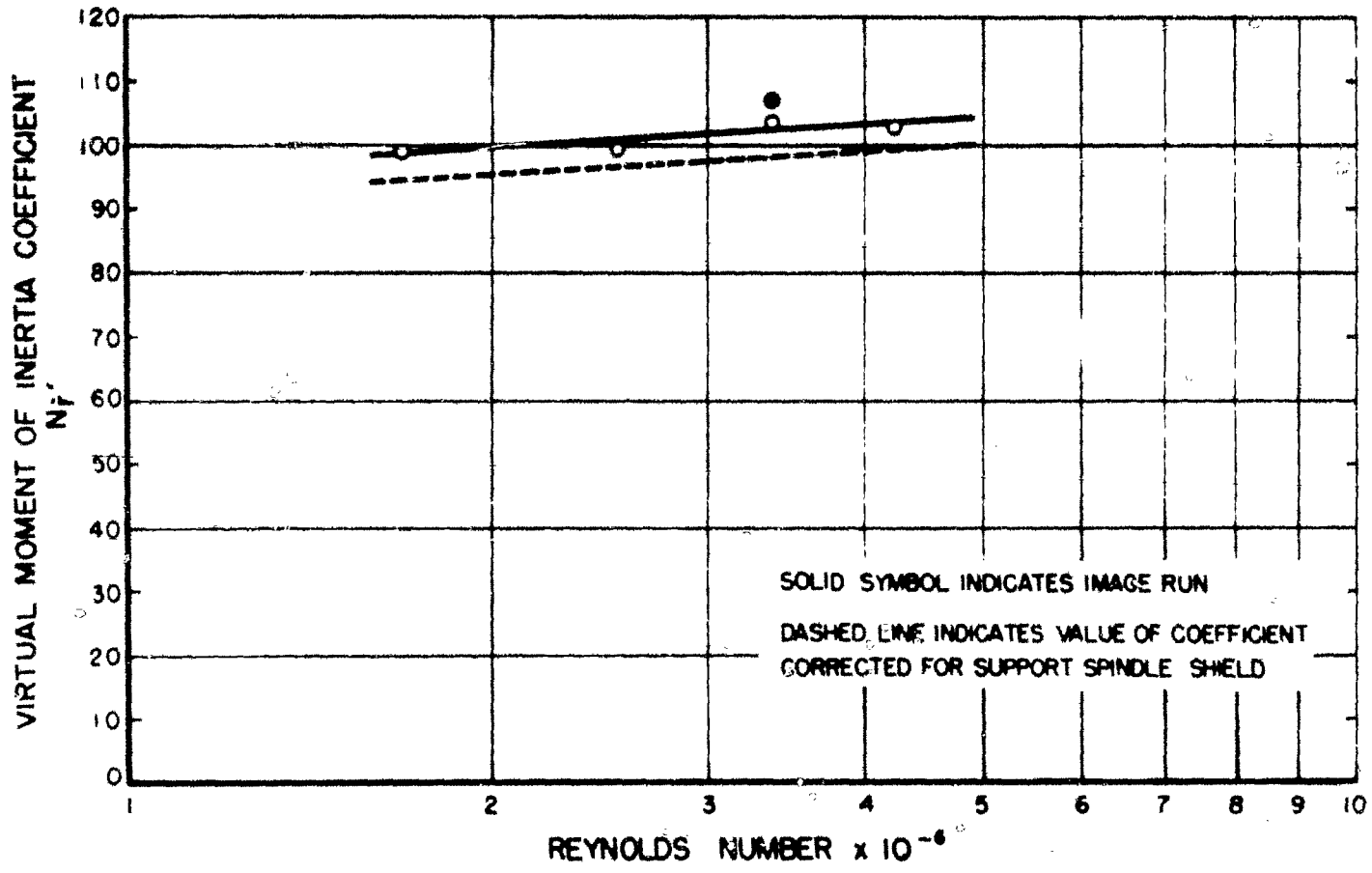

Fig. 7 - Virtual moment of inertia coefficient (angular acceleration) as a function of Reynolds number.

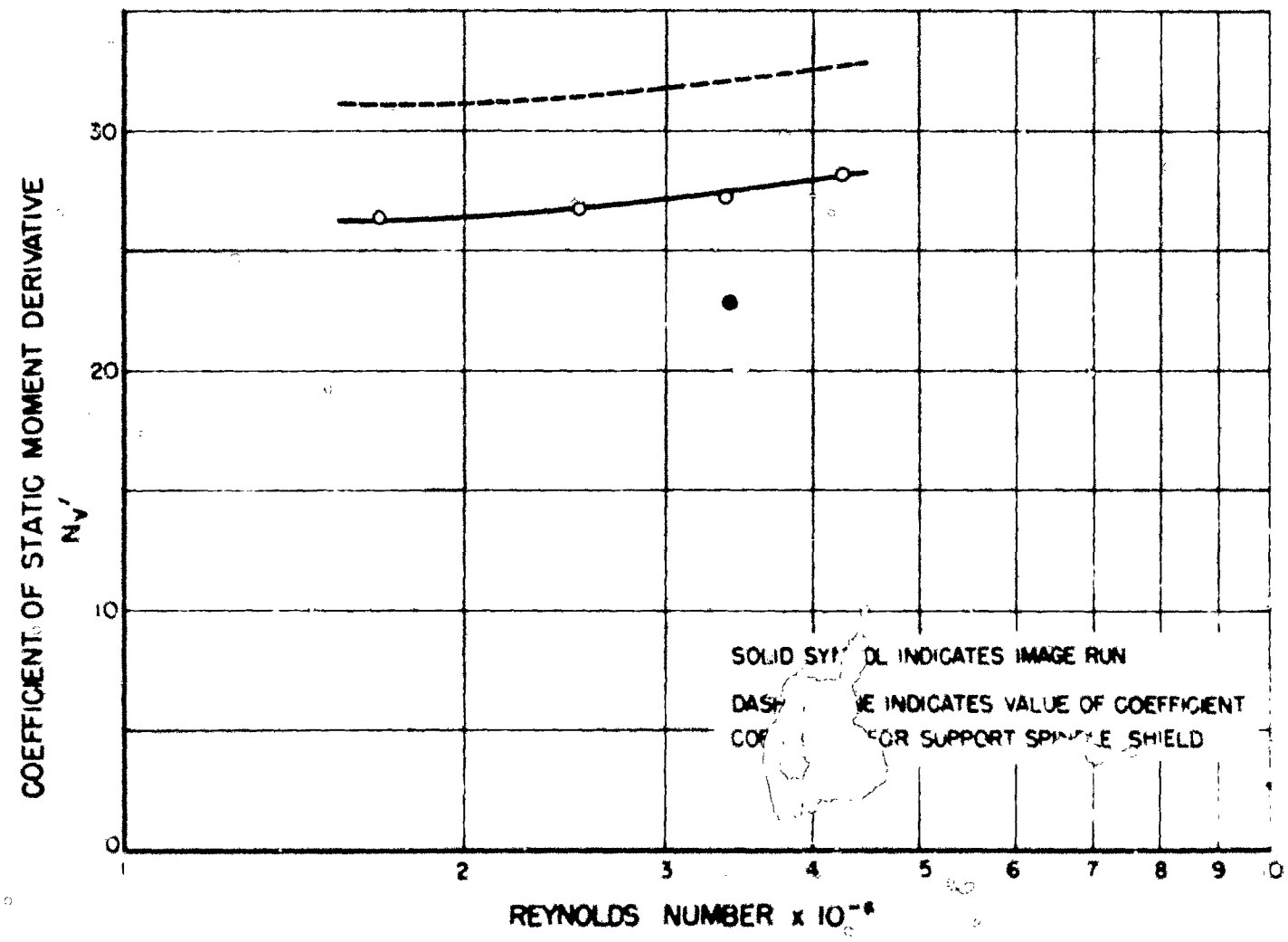

Fig. 8 - Coefficient of static moment derivative as a function of Reynolds number.

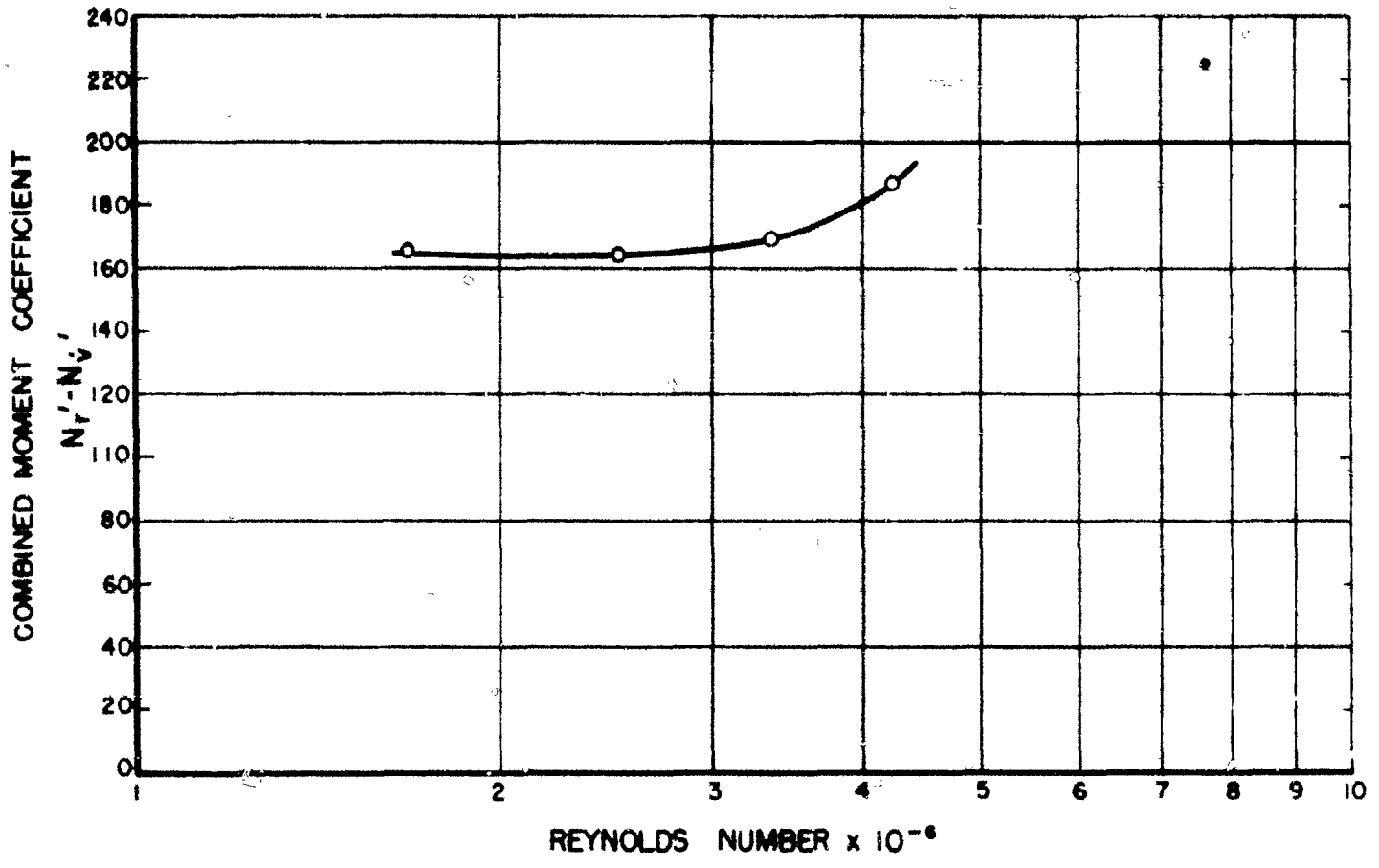

Fig. 9 - Combined moment coefficient as a function of Reynolds number.

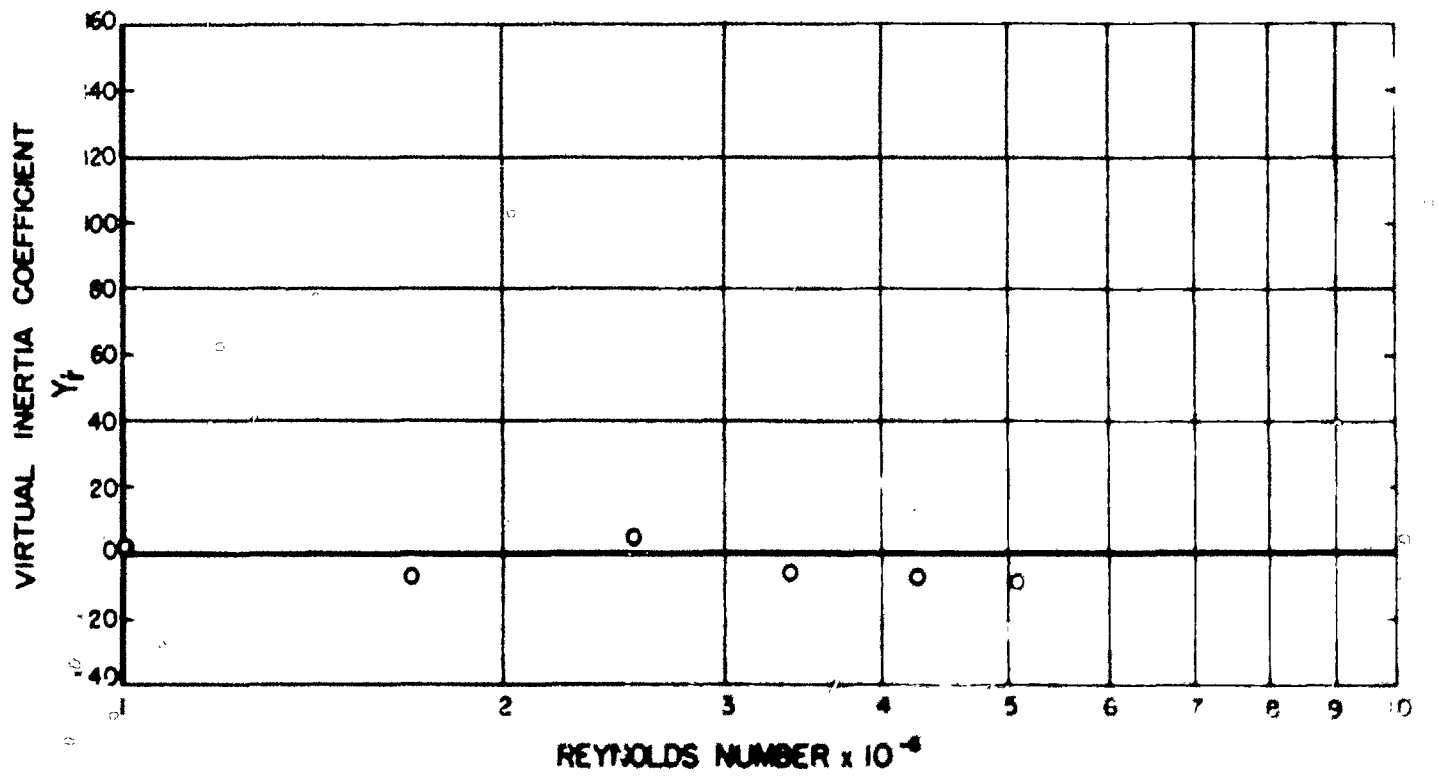

Fig. 10 - Virtual inertia coefficient (angular acceleration) as a function of Reynolds number.

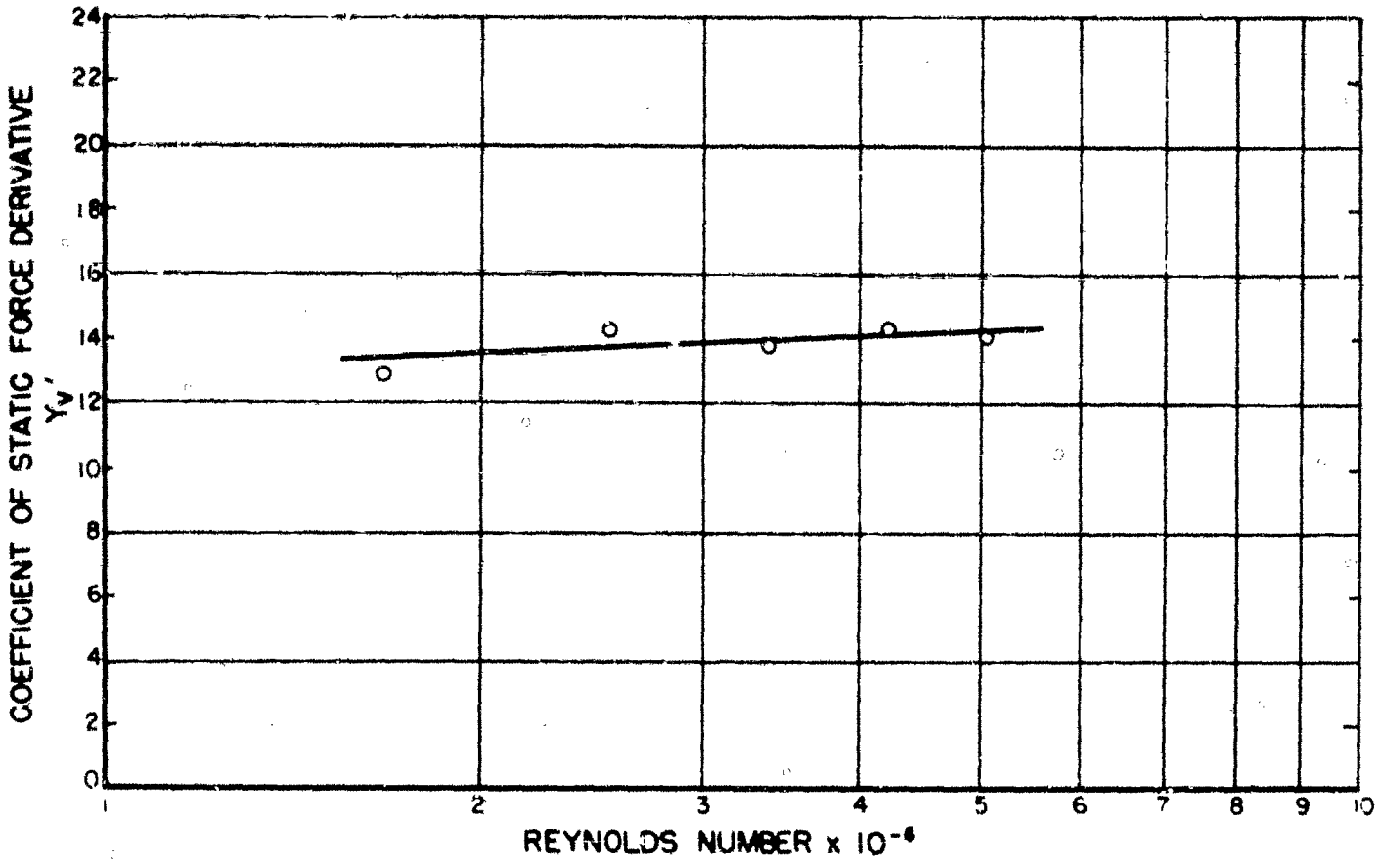

Fig. 11 - Coefficient of static force derivative as a function of Reynolds number.

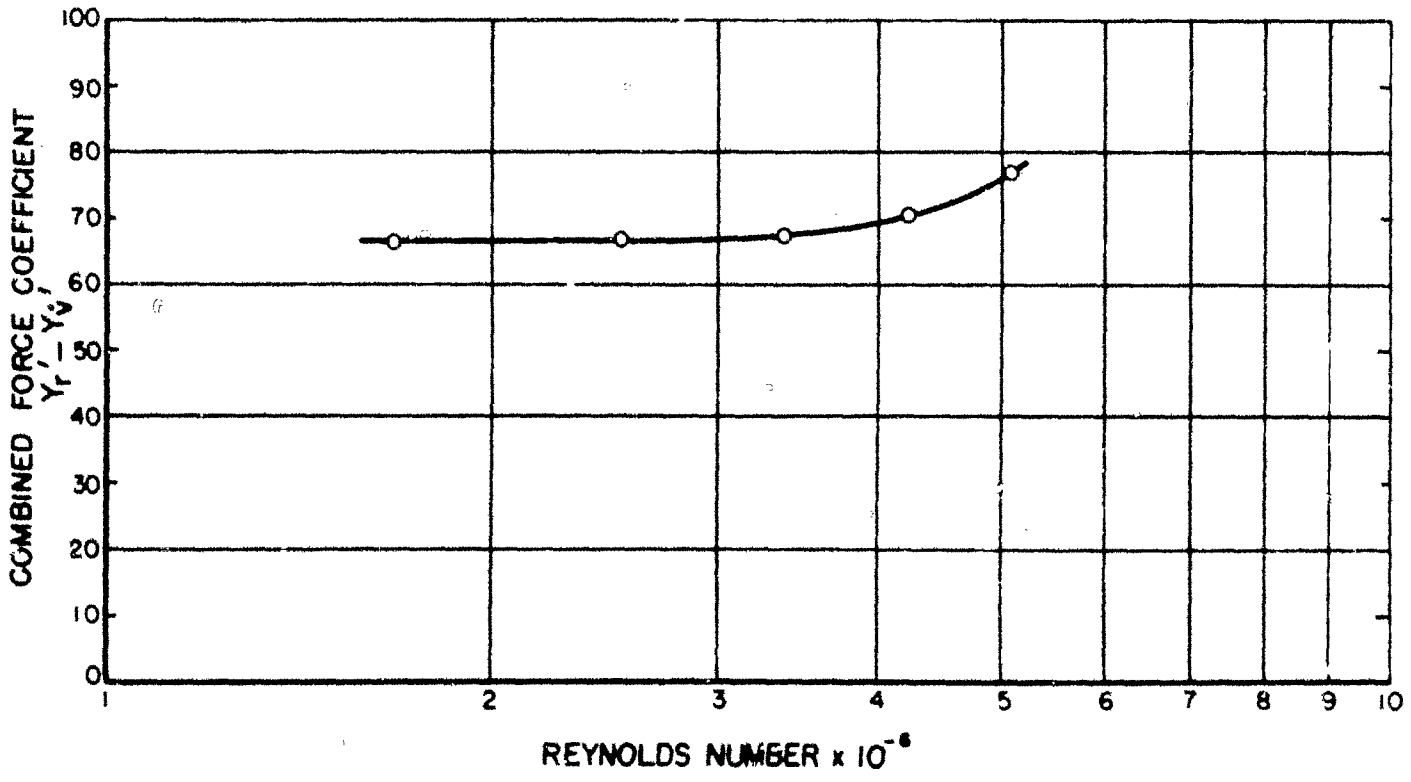

Fig. 12 - Combined lateral force ccefficient as a function of Reynolds number.

DISTRIBUTION LIST

Copy No.

1-4 Chief, Bureau of Ordnance, Navy Dept., Washington 25, D. C.
Attn: Code ReO-3

5-8 Chief, Bureau of Ordnance, Navy Dept., Washington 25, D. C.
Attn: Code ReU

9-10 Chief, Bureau of Ordnance, Navy Dept., Washington 25, D. C.
Attn: Code Ad3

11-13 Chief, Bureau of Aeronautics, Navy Dept., Washington 25, D. C.

14-18 Chief, Bureau of Ships, Navy Dept., Washington 25, D. C.

19-21 Chief, Office of Naval Research, Navy Dept., Washington 25, D. C.
Attn: Code 438

22 Commanding Officer, Office of Naval Research Branch Office,
1030 East Green Street, Pasadena 1, California

23-24 Commanding Officer and Director, David Taylor Model Basin,
Washington 7, D. C.

25-26 Commanding Officer, U. S. Naval Underwater Ordnance Station,
Newport, Rhode Island

27-28 Commander, U. S. Naval Ordnance Laboratory, White Oak,
Silver Spring, Maryland

29-30 Commander, U. S. Naval Ordnance Test Station, Pasadena,
California

31 Commander, U. S. Naval Ordnance Test Station, China Lake,
California

32 Director, Experimental Towing Tank, Stevens Institute of
Technology, via: Bureau of Aeronautics Representative
c/o Bendix Aviation Corp., Eclipse-Pioneer Division,
Teterboro, New Jersey

33 Director, Ordnance Research Laboratory, Pennsylvania State
University, University Park, Pennsylvania

34 Alden Hydraulic Laboratory, Worcester Polytechnic Institute,
Worcester, Mass., via: Inspector of Naval Material,
495 Summer Street, Boston 10, Mass.

35-36 Librarian, U. S. Naval Postgraduate School, Monterey, Calif.

DISTRIBUTION LIST (cont'd)

Copy No.	
37-46	British Joint Services Mission, Navy Staff, via: Chief, Bureau of Ordnance, Navy Dept., Washington 25, D. C., Attn: Code Ad8
47-49	Commander, U. S. Naval Proving Ground, Dahlgren, Virginia
50-51	National Advisory Committee for Aeronautics, Langley Memorial Aeronautical Laboratory, Langley Field, Virginia
52	National Advisory Committee for Aeronautics, Lewis Flight Propulsion Lab., Cleveland Airport, Cleveland, Ohio
53	Director, National Advisory Committee for Aeronautics, 1512 H Street, N. W., Washington 25, D. C.
54	Director, National Advisory Committee for Aeronautics, Ames Laboratory, Moffett Field, California
55-56	Commander, Air Research and Development Command, Post Office Box 1395, Baltimore 3, Maryland
57	ASTIA Reference Center, Technical Information Division, Library of Congress, Washington 25, D. C.
58-63	Director, Armed Services Technical Information Agency, Documents Service Center, Knott Building, Dayton 2, Ohio. Attn: DSC-SA